Journal of Applied Sciences and Nanotechnology

Journal homepage: jasn.uotechnology.edu.iq

Applying Ni-WC as a Composite Coating Combines both Protective and Repair Functions by Thermal Spray for HPTB Applications

[1]Alaa Zamel Dahesh*, [1]Ahmed Mohammed Hassan, [2]Hussain Mohammed Yousif

[1]College of Materials Engineering, University of Technology-Iraq, Iraq
[2]State Company for Steel Industries, Ministry of Industry and Minerals, Iraq

ARTICLE INFO

Article history:
Received: August, 01, 2025
Accepted: December, 05, 2025
Available online: December, 05, 2025

Keywords:
Coating,
Repair,
High pressure turbine blades,
Flame thermal spray,
Taguchi

Corresponding Author:
Alaa Zamel Dahesh
mae.22.028@grad.uotechnology.edu.iq

ABSTRACT

This work presents a solution to repair the deteriorating High-Pressure Turbine Blades (HPTB) instead of costly replacement by implementing a two-coating layer system for protection and repair. The first layer is a Bonding Coating (BC) that is made from a nickel-based alloy (NiCrBSi); the second layer is a Top Coating (TC), which is composed of a nickel-based composite material that contains tungsten carbide (WC) particles. Both layers were applied to a nickel-based substrate using a flame thermal spraying (FTHS) technique, with the spray parameters chosen based on the Taguchi method. The results were analyzed using optical microscopy, scanning electron microscopy (SEM), and energy-dispersive X-ray spectroscopy (EDS). The findings indicated that a coating layer with a thickness of 200–300 μm was successfully deposited using the FTHS method. The optimal spraying parameters determined by the Taguchi method were: a spraying distance (SOD) of 150 mm, a feed rate (FR) of 30 g/min, and a transverse velocity (TV) of 300 mm/min. Among these factors, SOD was identified as having the greatest influence on the spraying process, followed by FR, and then TV. A crack area on HPTB was successfully repaired using an improved FTHS process, resulting in a homogeneous, dense, and crack-free structure.

https://doi.org/10.53293/jasn.2025.7912.1351, Department of Applied Sciences, University of Technology - Iraq.

1. Introduction

Damage to the parts that operate at high temperatures exceeding 1000 °C is a common issue, particularly in gas turbine engines. In these engines, thermo-mechanical stresses occur in the rotor blades of the high-pressure turbine blades (HPTB) unit due to the combination of high pressure and high temperatures. Damage occurs at the leading edges (LE) or trailing edges (TE) or the blade tips during service [1, 2]. The causes of turbine blade damage can be categorised into three main factors: operational, environmental, and impact-related. Operational factors include extreme temperatures, high pressures, and hard landings. Environmental factors may involve hot or polluted intake air. Impact-related damage can result from foreign object damage (FOD), such as dust and organic materials like birds, as well as engine debris, referred to as known object damage (KOD). **Fig. 1** illustrates the most common defects identified during HPT inspections using a borescope [3].

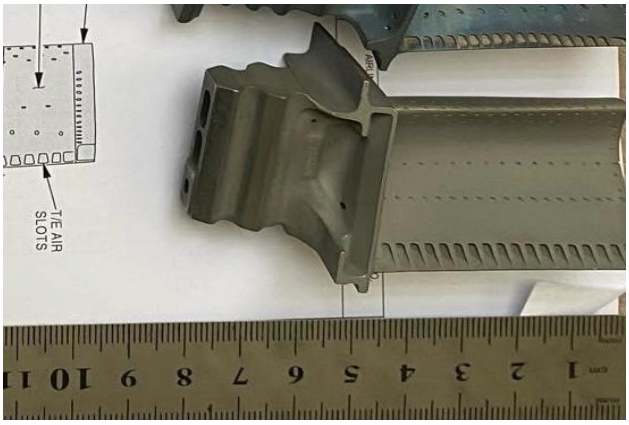

HPTB of the CFM56-72B engine

Oxidation/LE

Crack/LE

Burn through/LE

Missing material/Tip

Figure 1: Defects of HPTB.

Crucial materials used in aircraft engines, particularly for components such as turbine blades, discs, and other components in the hot core of the engine, are Ni alloys as shown in **Fig. 2**. Their properties make them well-suited for the demanding conditions of aircraft engines, which include high operating temperatures, high rotational speeds, and maintenance intervals averaging more than 3000 cycles, all while enduring oxidizing and corrosive environments [4, 5]. These alloys contain a face-centred cubic (FCC) γ-Ni matrix that contains cohesive mineral precipitates, borides, carbides, and other phases, including gamma prime (γ′). Various elements are added to improve the performance of the alloy: chromium and aluminium enhance oxidation resistance; cobalt, molybdenum, and tungsten increase high-temperature toughness; and carbon boosts creep resistance. One notable example of such an alloy is Inconel 718, which is widely used in the manufacture of turbine blades due to its

exceptional thermo-mechanical properties. To further enhance the reliability and durability of nickel alloys in severe environments, a protective coating layer is typically applied to prevent damage to the blades [6].

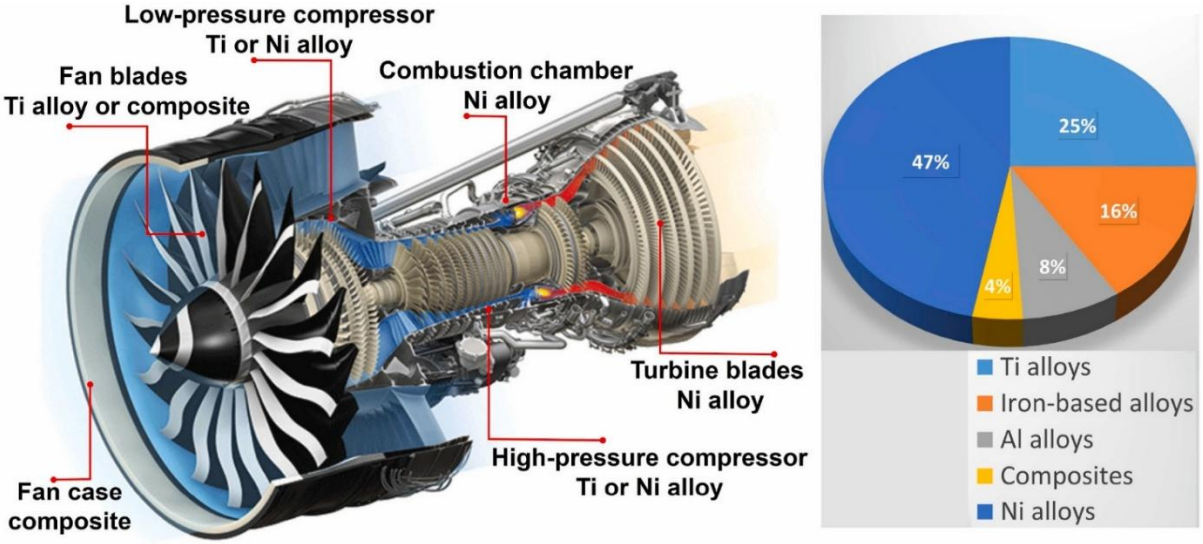

Figure 2: Materials used in General Electric's (GE's) turbofan engine for the Boeing [7].

In high-temperature applications, coatings typically have a 100–500 μm thickness and are applied in two coating layers. The top coating (TC) can be made of ceramic materials, such as YSZ (yttria-stabilised zirconia), or composite materials that include nickel with reinforcements like WC (tungsten carbide) or Al_2O_3 (alumina). The bonding coating (BC) is generally composed of metallic materials, such as NiCrAlY or NiCoCrAlY alloys [8-11].

Rather than replacing damaged components in gas turbine engines, such as blades, which can be costly and consume significant amounts of energy and environmental resources, these blades can be repaired and reused by employing efficient repair methods that maintain the blade's required standards, including dimensions, functional properties, and residual stress issues. Some of these repair methods include fusion welding [12], additive manufacturing [13, 14], and thermal spray [15]. Fiebig et al. attempted to repair HPTB by spraying different coating materials, e.g., Ni-based coating (IN718, IN738) and Ti-Al-Cr-Nb coating via cold spray (CS) and Vacuum Plasma Spray (VPS) methods. Results revealed that deposition coatings by the CS process are considered a challenge because of the high residual compression stresses formed in the coating layers. As well as the application of coating via VPS needs to have appropriate heat treatment (HT) along with it to create a coating with dense microstructure [16]. Nicholas et al. reformed HPTB of ENG via merged techniques: braze and Atmospheric Plasma Spray (APS), based on some steps: firstly, cleaning the damaged region, secondly, applying filler material (Ni650) using the brazing technique. Secondly, the application (MCrAlY) as BC and the Al layer as TC via the APS technique. Finally, the coated samples were specifically HT to ensure the best distribution among the coating layers, along with the IN718 substrate. They relied on a process of optimisation dependent on the DOE program to determine the best factors for spray coating materials with a diverse grain size. Based on SEM findings, it was found that the oxide percentage increases as the grain size decreases below 63 μm, and voids increase as the grain size increases above 63 μm. The latter problem can be treated via HT [17]. Le´tang et al. repaired the affected region in unserviceable HPTB by spraying a powder that has a chemical composition similar to that of the workpiece via a High Velocity Air Fuel (HVAF) technique. They concluded that the quality of the coating process is directly dependent on factors related to the spraying process itself, including the spray rate, nozzle-to-substrate distance, nozzle size, and coating powder size. They also concluded that the spray distance played a key role in determining the properties of the coating layer, including porosity and resulting oxides [18]. Donnini et al. reviewed a landmark study on the repair of nickel-based alloys, such as Inconel 718, used in turbine applications, using conventional welding methods, such as high-energy welding (laser or electron beam). Although these methods are effective in repairing damaged parts at high speed, several factors, including the varying chemical composition of the weld materials and substrate, lead to crack formation in the heat-affected zone (HAZ) of the processing area. This remained a significant problem in welding processes [12].

Among various coating methods, and with the help of many effective auxiliary techniques, such as Taguchi design [19] or appropriate heat treatment [20], Flame thermal spraying (FTHS) is considered a reliable and effective technique for depositing hard coatings. This method produces coatings with low porosity, free from cracks, good resistance to thermal shock, and effective protection against wear and erosion, all in a cost-effective manner when compared to other more expensive and complicated techniques like cold spray, plasma spray, HVAF, and additive manufacturing (AM). Fanicchia et al. applied bond coating BC and top coating TC using two different processes: FTHS and APS. In their work, a comparative study was conducted between these coating processes. By examining the characteristics of the final resulting coating, porous and oxide content, micro-hardness, and thermal shock tests. They inferred that although the microstructure of coating formed by the FTHS process contains porosity and harmful oxide, it remains less complicated and less costly, and produces a layer with thermal shock resistance higher by 80% than the APS process, and this refers to the efficiency of FTHS in preparing these layers [21]. Frunzaverde et al. concluded from their work that using FTHS along with HT (e.g. remelting) contributed to reducing the FTHS disadvantages represented by high porosity. They deposited NiCrBSi powder as BC, followed by NiCrBSi mixed with 20% (WC-Co) as TC. Then, the coatings were exposed to the flame of oxygen-acetylene to remelt them to ensure complete interdiffusion between TC/BC and BC/substrate layers. According to the results, this study achieved coating with good hardness that serves a protective function against wear and corrosion factors [15].

In addition to various HPTB repairing methods, the selected materials for the repair process are a subject of scientific and industrial fields. These materials include cermet [20], superalloys [22], ceramic [23], and intermetallic [24]. Chaudhary et al. reported that ceramic coating materials, such as yttria-stabilised zirconia (YSZ), performed as thermal insulation coatings when applied to HPTB. They often do not adhere effectively to the substrate and thus peel off easily when subjected to thermal shock testing. This is due to differences in mechanical properties and coefficients of thermal expansion (CTE) of the two coating materials. For example, the CTE of nickel-based alloys is approximately 14 × 10-6 °C, while that of ceramic materials is lower. Therefore, the use of metal matrix composites (MMCs), which include metal alloys reinforced with ceramic particles, as coating materials can provide better compatibility with the metal substrate [25]. The promising solution for reducing thermal expansion mismatch between coating layers is the use of metal matrix composite (MMC) coatings. Rashidi et al. mixed 60% tungsten carbide (WC) with Ni-based powder to prepare a composite coating, which was applied by FTHS. Depending on characteristic tests such as optical microscopy and SEM, and mechanical tests such as Vickers hardness and wear tests. A cohesive layer with strong adhesion, less porosity, and acceptable wear resistance was acquired. They found that the addition of WC as a hard phase, together with other hard phases such as borides and carbides, led to an improvement in the mechanical properties of the coated samples [26]. Harith et al. showed that adding tungsten carbide and cobalt in specific proportions to nickel to fabricate a composite coating and spraying it onto an IN718 substrate by thermal spraying helped improve the erosion resistance of the coated sample [27]. This study aimed to use the same coating process and materials to repair damaged turbine blades. Using flame thermal spraying technology, two layers were applied: the first was a nickel alloy powder (NiCrBSi) used as a bond layer, and the second was a composite coating (Ni-WC) as a top layer. The optimum thermal spray parameters were determined using Minitab to obtain a dense coating with minimal gaps and high adhesion strength. The results were analysed and discussed using optical microscopy (OM), energy-dispersive X-ray spectroscopy (EDS), and scanning electron microscopy (SEM).

2. Used Materials

The specimens used in this study were Inconel 718 alloy, consisting of flat specimens with dimensions (1×1× 0.04) cm. To improve the surface roughness, the samples were scratched with fine silica. Following, they were cleaned in an ultrasonic bath using isopropanol. This study utilised two types of powders as repair and protection materials, as shown in **Fig. 3a, b.** The first powder, referred to as BC, was made up of NiCrBSi (brand name 10009 Eutalloy, USA) with particle sizes ranging from 20 μm to 97.2 μm. The second powder, known as TC (top coating), comprised Ni-WC (brand name 10112 Eutalloy, USA) with particle sizes ranging from 42.86 μm to 93.31 μm. The chemical compositions of the used materials are presented in **Table 1**.

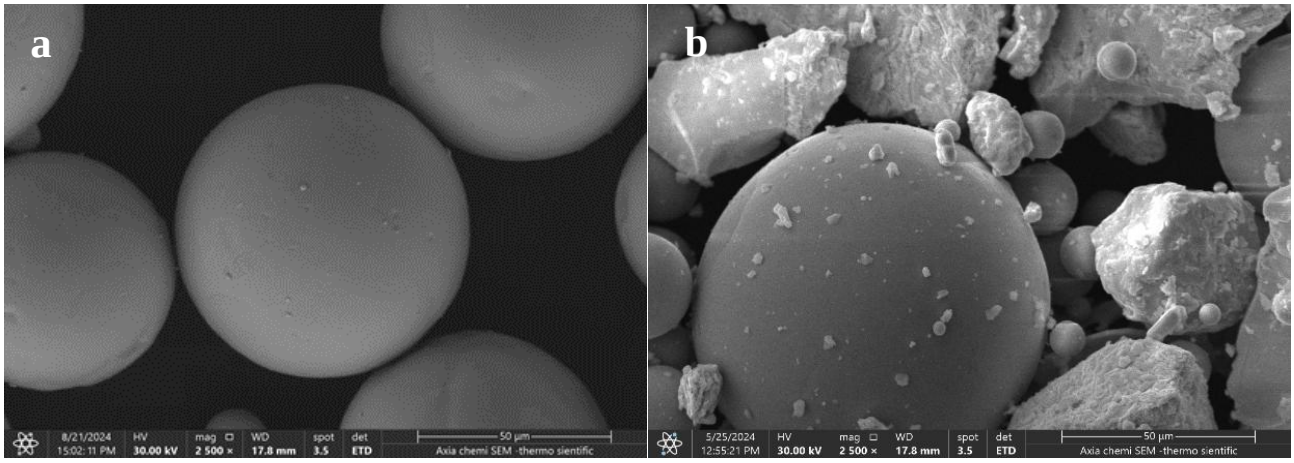

Figure 3: SEM images **a**) BC and **b**) TC powders.

Table 1: Chemical composition (%) by weight of substrate and powder of coating.

Materials	Ni	Cr	Al	Fe	C	Hf	B	Si	W
Inconel718 (substrate)	Base	17.12	0.5	18.5	0.07	-	0.04	0.31	-
NiCrBSi (BC)	Base	13.0	0.32	3.6	-	-	1.1	5.07	-
Ni based-WC(TC)	Base	5.11	0.21	3.2	0.11	0.1	0.07	2.21	27.1

3. Experimental Procedure

3.1. Flame Thermal Spraying (FTHS) Technique

The coating used for protection and repair purposes was applied by flame thermal spraying. A SuperJet Eutalloy spray gun (SuperJet Eutalloy, Castoline Eutectics) was automatically supplied with a gas mixture consisting of oxygen at 0.5 bar and acetylene at 0.7 bar, as shown in **Fig. 4**. The spray gun is mounted on the x-axis, assisted by a ball-bearing trowel for horizontal back-and-forth movement. The sample to be coated is held on the y-axis by a clamp and a ball-bearing trowel for vertical movement. The movement of the gun and sample is automatically controlled to ensure a uniform coating process. After the oxygen-acetylene gas mixture is burned (the flame temperature reaches 3000 °C), the coating particles supplied through an orifice at the top of the spray gun are heated to temperatures close to their melting point and then sprayed at high speed by hot compressed gases. These particles exit the nozzle and collide with the substrate surface. These thermal collisions continue until the coating layer is deposited. **Fig. 5** shows coated and uncoated samples.

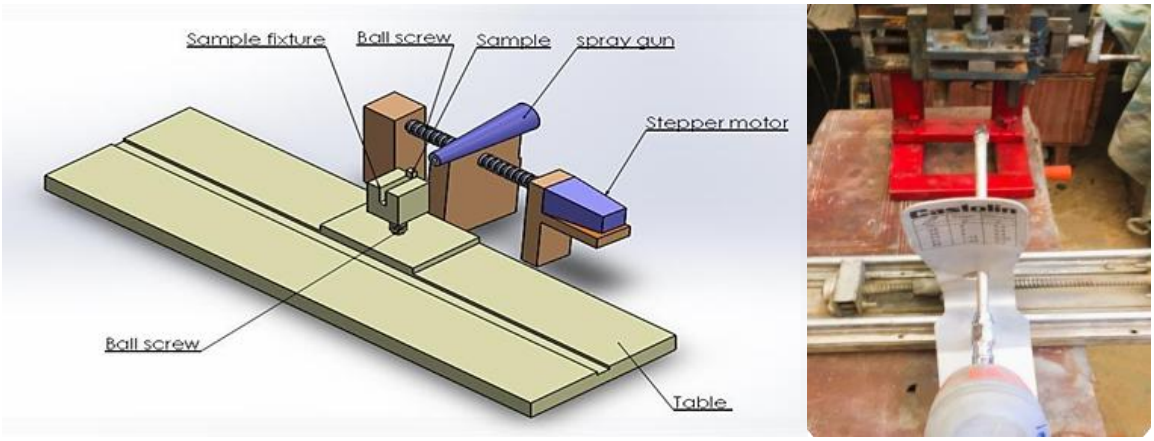

Figure 4: Set up of FTHS rig.

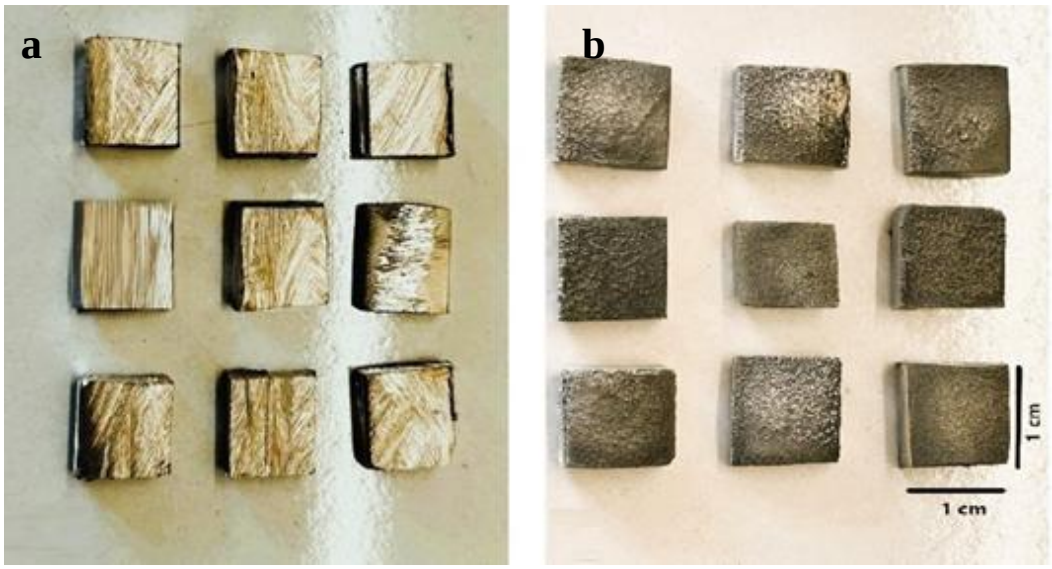

Figure 5: Photograph images for specimens **a**) uncoated, **b**) coated.

3.2. Numerical Optimisation via Taguchi

Previous studies and tracking experiments indicate that producing high-quality thermal spray coatings requires a suitable design of experiments (DOE). One useful tool for this is the Minitab software for DOE. In these experiments, spray parameters such as standoff distances SOD, mm), transverse velocity TV, mm/min), and feed rates FR, g/min) are selected at various levels, as detailed in **Table 2**. The chosen spray parameters are then organised at different levels using the Taguchi L9 (3^3) orthogonal matrix, as shown later in the results section.

Table 2: Factors and levels of the Flame thermal spraying technique.

Parameter	Units	Code	Levels		
			1	2	3
SOD (Standoff distance)	mm	A	100	125	150
TV (Traverse Velocity)	mm/min	B	100	200	300
FR (Feed Rate)	g/min	C	10	20	30

Prior research has determined that medium spray distances ranging from 100 mm to 150 mm are optimal for depositing high-quality, low-porosity coatings. A study by Miftah et al. demonstrated a decrease in adhesion strength when the standoff distance exceeded the intermediate range of 200 mm to 300 mm [28]. Additionally, Mrdak et al. found that using standoff distances below the medium range from 80 mm to 120 mm led to less effective layer formation [29].

Where the S/N equation used in this research is the bigger is better, as shown in Eq. (1):

$$\mathbf{S/N} = -\mathbf{10}.\log_{10}\left(\frac{\Sigma\left(\frac{1}{Y^2}\right)}{n}\right) \quad (1)$$

In this study, the response variable is denoted as Y (the depth of diffusion), and n represents the number of replications of the experiment, which is set as three replications.

3.3. Devices Used in Microstructural Characterisation

The depth and thickness of the coating diffusion were measured using a 40X magnification optical microscope, using a MEIJI Techno microscope. A scanning electron microscope equipped with energy-dispersive X-ray spectroscopy (EDX), specifically the Thermo Scientific™ Axia ChemiSEM™, was utilised to evaluate the surface morphology and cross-section of the coatings. This analysis aimed to investigate the porosity, interface area, and chemical composition of the coated samples.

3.4. HPTBs Repair

The FTHS process was used to repair a turbine blade that had a tip crack. To facilitate this process, an artificial crack less than 0.05 cm was created in four samples measuring (2 × 2 × 0.04) cm, designed to mimic the shape of the blade tip. To repair the HPTB, the crack area at the blade tip was first cleaned. Following this, two layers of coating were applied using FTHS along with the optimal parameters. A spray nozzle with a diameter of 0.5 mm was used to concentrate the coating materials in a narrow area. To protect the remaining parts of the turbine blade during the spraying process, a piece of alumina was employed as a shield, as illustrated in **Fig. 6**.

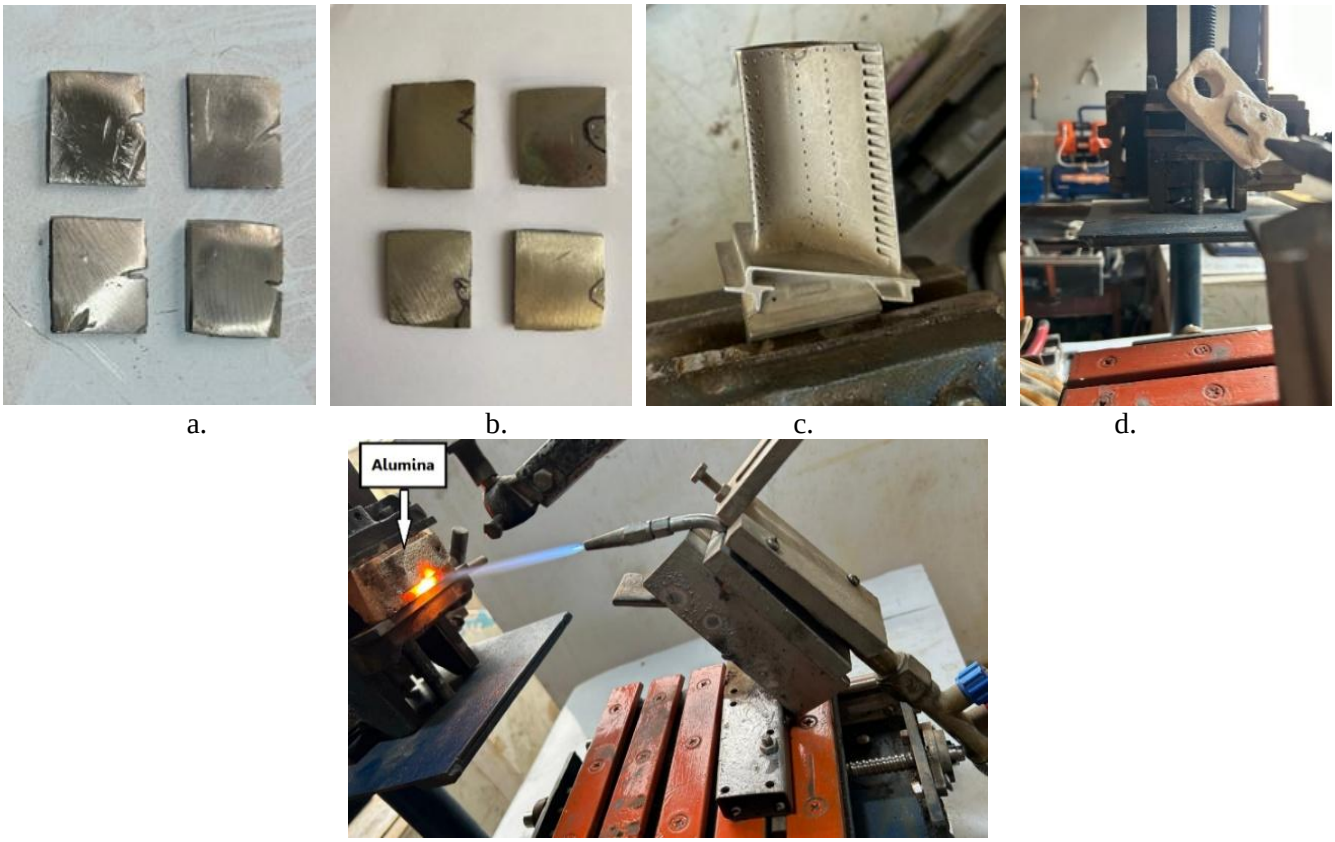

Figure 6: a) samples before repair, **b**) samples after repair, **c)** HPTB after repair, **d**) protective shield Alumina, e) using the FTHS technique for repair.

4. Results and Discussion

4.1. FTHS Parameters Optimisation via Taguchi

Nine testing operations were performed according to the proposed design, according to the Taguchi method, and the depths of penetration in mm are Trial1, Trial2, and Trial 3.

The results tabulated in **Table 3** indicate that the greatest spread was achieved in round 7, characterised by an SOD of 150 mm, a TV of 100 mm/min, and a FR of 30 g/min. It was observed that with the largest and lowest signal-to-noise values, the disturbance rate was low.

To determine which parameters, require control to achieve coating with good properties, a response table of means and signal-to-noise ratio (S/N) was utilised. The parameter with the largest difference in delta value, defined as the difference between the highest average S/N and the lowest average S/N for each parameter, exerts the most significant influence on the response. The results indicate that SOD (A) had the highest effect and delta value, making it the parameter with the greatest influence on coating spread (ranked 1st). In contrast, TV (B) had the least influence among the other parameters (ranked 3rd), as shown in **Tables 4** and **5**. Based on these results, **Fig. 7** shows the mean and S/N plots generated using Minitab software.

Table 3: Results of Taguchi Orthogonal Matrix (OA)-L9.

Code	A	B	C	Trial1	Trial2	Trial3	Mean	S/N
1	100	100	10	51	53	48	50.66	34.09
2	100	200	20	66	64	61	63.66	36.08
3	100	300	30	67	69	67	67.66	36.61
4	125	100	20	47	48	44	46.33	33.32
5	125	200	30	55	53	54	54	34.65
6	125	300	10	64	58	60	60.66	35.66
7	150	100	30	72	71	72	71.66	37.11
8	150	200	10	66	68	65	66.33	36.43
9	150	300	20	59	56	61	58.66	35.37

Table 4: Response for means.

Level	A	B	C
1	60.67	56.22	59.22
2	53.67	61.33	56.22
3	65.56	62.33	64.44
Delta	11.89	6.11	8.22
Rank	1	3	2

Table 5: Response for S/N.

Level	A	B	C
1	35.59	34.84	35.40
2	34.54	35.72	34.92
3	36.30	35.88	36.12
Delta	1.76	1.04	1.20
Rank	1	3	2

From **Fig. 7**, the diffusion depth increased over 10 µm when the SOD was raised from 125 mm to 150 mm. Additionally, an increase in the FR from 20 g/min to 30 g/min resulted in an improvement of about 8 µm in diffusion depth. Furthermore, the diffusion depth also increased over 6 µm when the TV was increased from 100 mm/min to 300 mm/min. So, the optimal coating conditions were achieved by selecting the following parameters: A3 (SOD = 150 mm), B3 (TV = 300 mm/min), and C3 (FR = 30 g/min), as appear in **Table 6.**

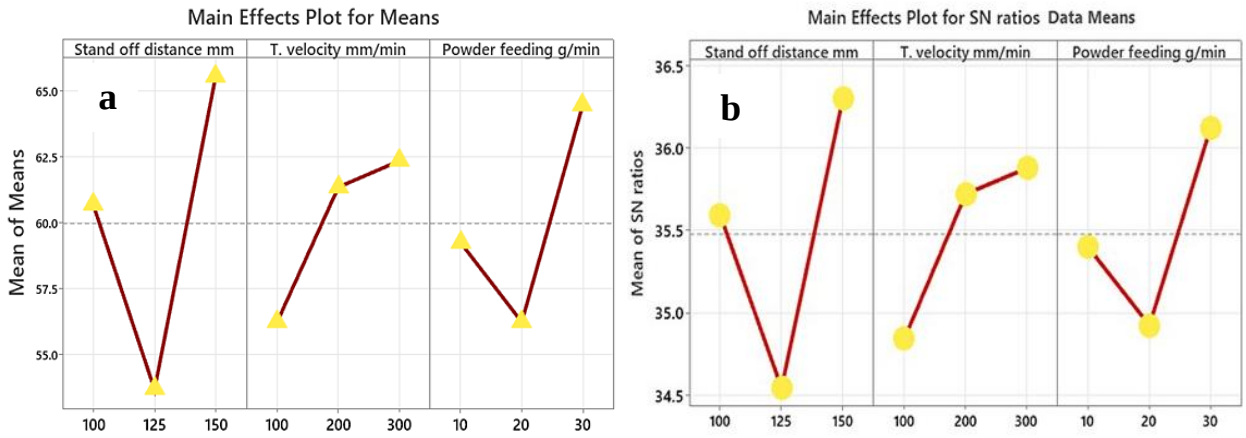

Figure 7: Diffusion main effect plot for: **a**) means and **b**) S/N.

Table 6: Optimization of the experiments conducted via Taguchi.

Factor	A	B	C
Level	3	3	3

The analysis of variance (ANOVA) combined with the Taguchi method is one of the most widely used statistical techniques for studying experimental results and determining the impact of each factor. As illustrated in **Table 7**, the results based on the Taguchi and ANOVA indicate that parameter A (SOD) has the greatest influence on the diffusion value, with an effect of 37.64%. This is followed by parameter C (FR), which contributes 17.4%, and parameter B (TV) with 15.01%.

Table 7: ANOVA for S/N ratio.

Source	DF	Seq SS	Adj SS	Adj MS	F	P	Contribution%
SOD (A)	2	4.71	4.71	2.35	1.26	0.44	37.64
TV (B)	2	1.87	1.87	0.93	0.50	0.66	15.01
FR (C)	2	2.18	2.18	1.09	0.59	0.63	17.40
Residual-Error	2	3.73	3.73	1.86			29.85
Total	8	12.51					100

DF: degrees of freedom, SS: sum, MS: mean squares (Variance), F: ratio of a source variance to error variance, $P < 0.05$ determines significance of a factor at 95% confidence level

4.2. Coated Samples Characterisation

Fig. 8a and b displayed the coated samples along with their cross-sections. The typical coating layers, consisting of an interdiffusion zone (IDZ), a bonding coating (BC), and a top coating (TC), are formed. The average total coating thickness ranged from 200 μm to 300 μm. The results from SEM and EDS are presented in **Fig. 9**. The surface and cross-section of the coated sample are depicted in Fig. 9a and b. As observed, the coating layers were applied to the substrate continuously and uninterruptedly, without any microcracks at the interface. This success can be attributed to the optimal spraying conditions established following the Taguchi method. The coatings exhibit high density and a homogeneous microstructure, with spherical particles ranging in size from 300 nm to 1.6 μm. This finding confirmed the complete dissolution of most coating materials, which are deposited uniformly on the substrate with a porosity of less than 4%. The EDS results indicate the presence of all coating elements, as shown in **Fig. 9c**.

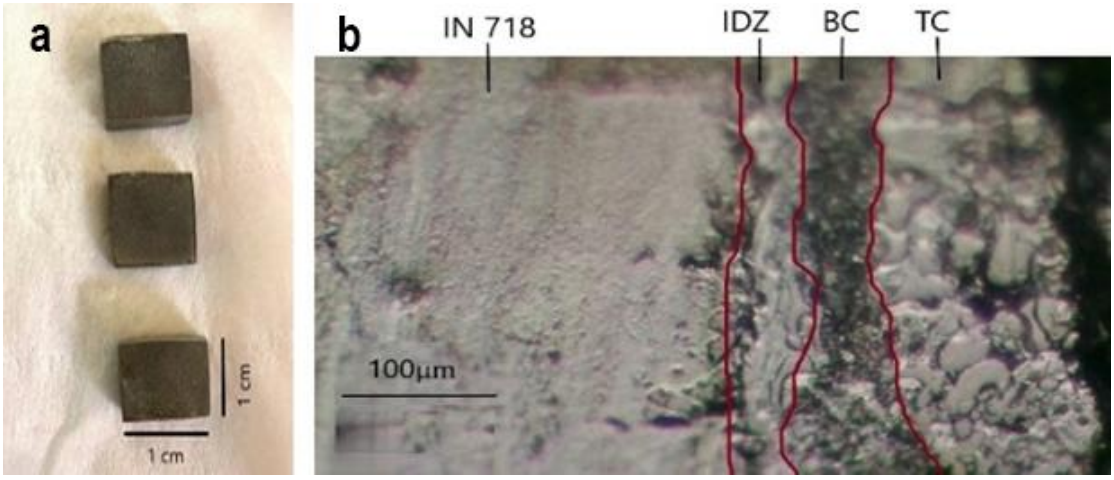

Figure 8: a) Optimise Samples, **b**) diffusion depth of the coating using optical microscopy.

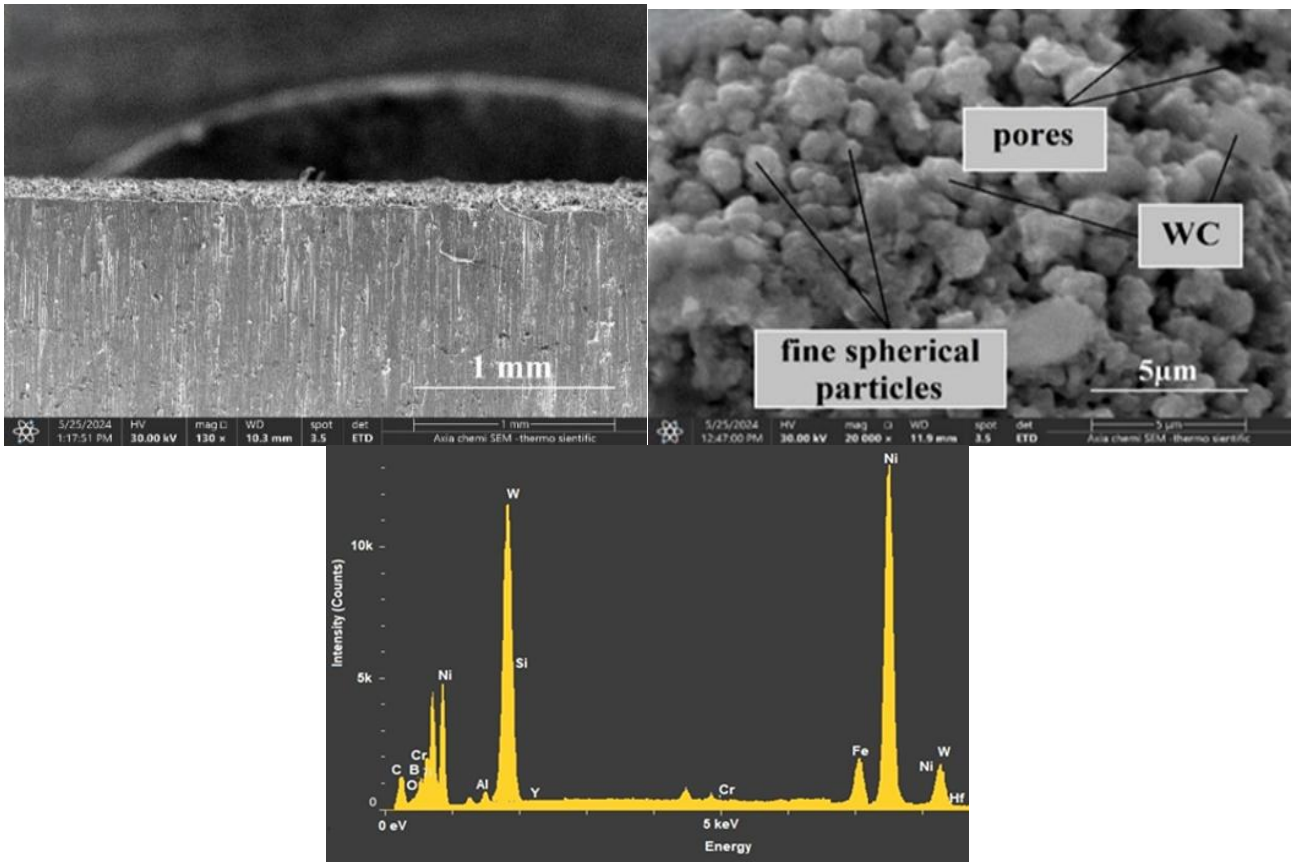

Figure 9: SEM images of coated samples: **a**) cross-section; **b**) surface; c) EDS results of the coating layer.

4.3. HPTB Repair

Cracking is a major challenge faced when repairing gas turbine blades using conventional methods like welding and laser treatment, as illustrated in **Fig. 10**. This problem occurs when cracks appear after the repair material has solidified. The rapid heating and cooling cycles create thermal gradients within the blade material. These gradients induce stresses that can persist even after the material has solidified. If these stresses exceed the strength of the material, cracks develop [30, 31]. EDS-SEM analysis results of the repaired HPTB showed high-resolution images of the fracture area repaired by thermal spraying and the distribution of elements at specific locations (between the blade area and the repair material), which helped in determining the quality and properties of the deposited layers, in terms of the appearance of pores, microscopic cracks and oxidation products. Chemical composition of the HBTB showed in **Table 8**.

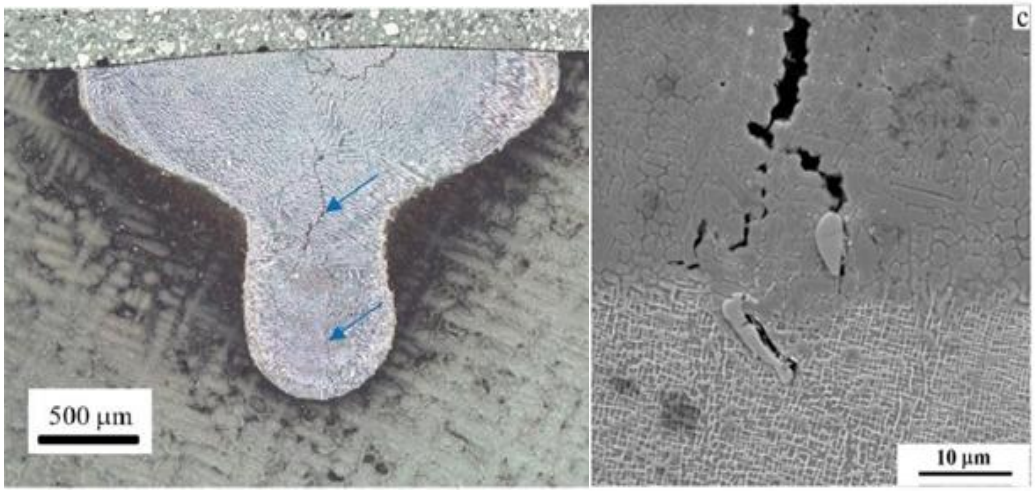

Figure 10: The structure of samples after repair by laser melting [30].

Table 8: Chemical composition of the HBTB (substrate).

Materials	Ni	Cr	Al	Fe	C	*Co*	B	Si	Y	Ta	Mo	W
HPTB (substrate)	Base	5.2	3.8	8.6	0.15	6.2	1.7	0.31	0.3	5.1	0.7	3.4

EDS analysis in **Fig. 11a and b** identified the chemical elements in the coating powder, as well as traces of Mo, Co, and Ta, which likely diffuse from the substrate into the coating material. Also, in **Fig. 11e**, the layers of the blade, BC, and TC, were displayed. The BC layer is a ductile material designed to protect the base material from cracking or damage when the outer coating containing hardened tungsten carbide particles is applied. The nickel-WC coating on the left side represents the functional surface, which acts as an erosion-resistant layer suitable for high-temperature environments. The EDS-SEM results show that the repair material was applied in a compact, layered manner within the crack area to ensure continuous alignment with the substrate structure. This approach created a dense region free of cracks and pores. In conclusion, the flame thermal spraying process offers significant advantages over traditional repair methods, such as ease of application and minimal thermal stress.

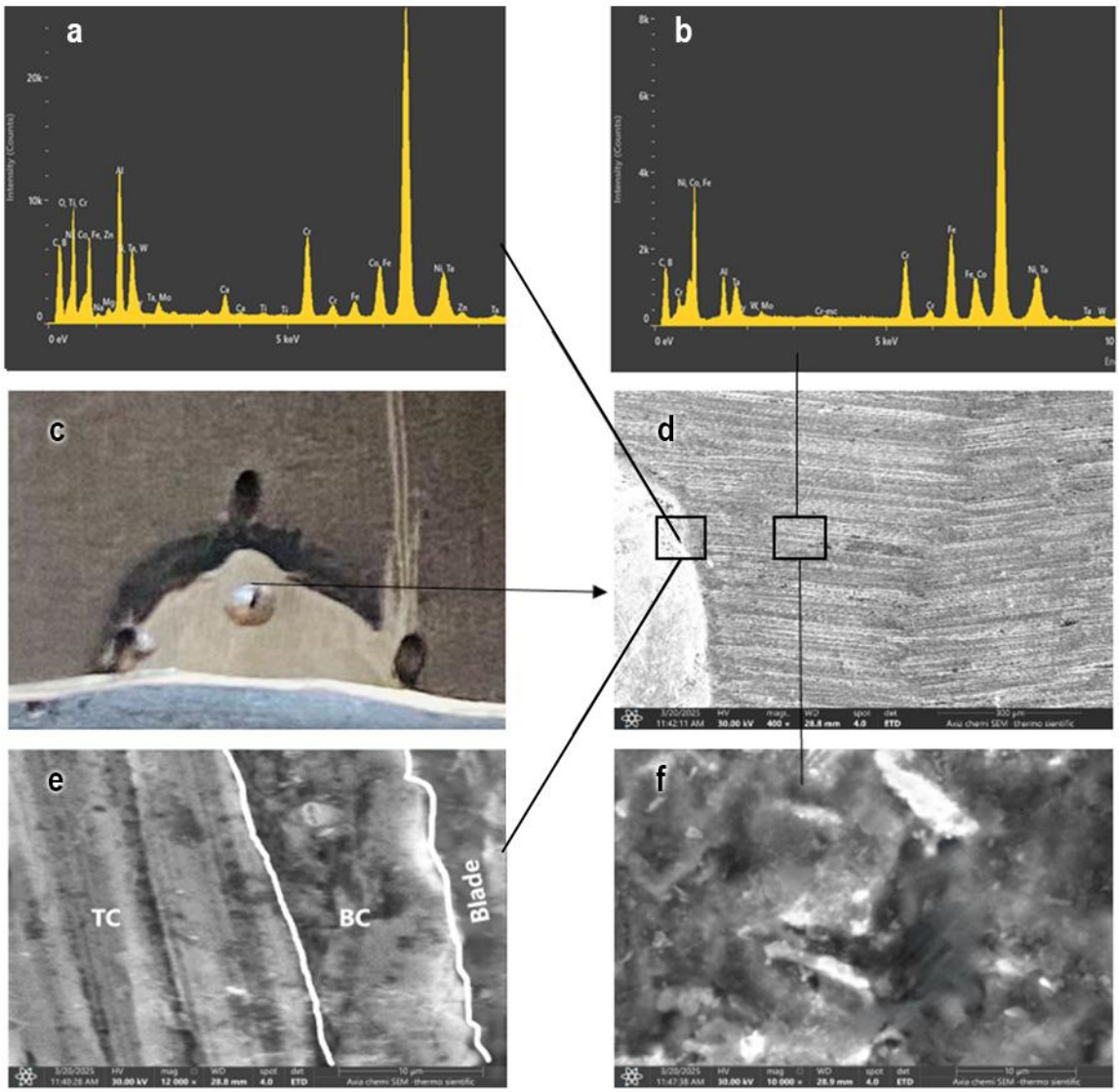

Figure 11: Microstructure of HPTB after repair, **a**) EDS of substrate/coating, **b**) EDS of blade, **c**) repaired HPTB at crack area, **d**) SEM of repair HPTB, **e**) SEM of substrate/coating, **f**) SEM of blade.

5. Conclusions

Experimental studies were carried out on samples coated with two layers as protective and repaired coatings. The first layer, known as the bonding coating (BC), was made of NiCrBSi powder. The second layer, referred to as the top coating (TC), consisted of Ni-WC and was applied to a nickel-based substrate using optimised flame thermal spraying. A coating with a thickness of (200-300) μm was successfully deposited using the FTHS method. The optimum FTHS parameters were selected according to the Taguchi method. They are as follows: SOD (150 mm), FR (30 g/min), and TV (300 mm/min). The most influential parameter in the spraying process was SOD, followed by FR, then TV. Based on optical microscope, SEM, and EDS tests, dense coating layers consist of a spherical particle structure with sizes ranging from 300 nm to 1.6 μm. FTHS processing is a promising method for repairing compact layers with minimal voids and no cracks.

Acknowledgement

The authors acknowledge University of Technology and the State Company for Steel Industries, Baghdad, Iraq, for their support.

Conflict of Interest

The authors declare that they have no conflict of interest.

References

[1] S. Zhu, Y. Li, J. Yan, and C. Zhang, "Recent Advances in Cooling Technology for the Leading Edge of Gas Turbine Blades," Energies, vol. 18, no. 8, 540, 2025. https://doi.org/10.3390/en18030540

[2] B. W. Lagow, "Materials Selection in Gas Turbine Engine Design and the Role of Low Thermal Expansion Materials," JOM, vol. 68, pp. 2770–2775, 2016. https://doi.org/10.1007/s11837-016-2071-2

[3] J. Aust, D. Pons, "Taxonomy of Gas Turbine Blade Defects," Aerospace, vol. 6, no. 58, 2019. https://doi.org/10.3390/aerospace6050058

[4] M. Bogdan, A. Kułaszka, D. Zasada, "The Impact of the Gas Turbine Blade Heating Temperature in the Presence of Aviation Kerosene on Coating and Alloy Microstructure," Acta Mechanica et Automatica, vol. 19, no.1, pp. 153-163, 2025. https://doi.org/10.2478/ama-2025-0018

[5] M. Tahari, F. Naeimi, "Effect of Surface Morphologies on the Isothermal Oxidation Behavior of MCrAlY Coatings Fabricated by High-velocity Oxyfuel Processes," International Journal of Engineering (IJE), TRANSACTIONS C: Aspects, vol. 30, no. 3, pp. 433-439, 2017.

[6] A. G. Muñoz, "Investigating the development of single crystal in the Ni-based Superalloy" IN718" by PBF-EB," MSc, Faculty of Science, Technology and Media, Department of Engineering, Mathematics, and Science Education, Mid Sweden University, diva-54324, Sweden, 2025.

[7] C. Tan, F. Weng, S. Sui, Y. Chew, G. Bi, "Progress and perspectives in laser additive manufacturing of key aeroengine materials," International Journal of Machine Tools and Manufacture, vol. 170, p. 103804, 2021. https://doi.org/10.1016/j.ijmachtools.2021.103804

[8] H. Liu, J. Cai, J. Zhu, "Hot Corrosion Behavior of $BaLa_2Ti_3O_{10}$ Thermal Barrier Ceramics in V_2O_5 and $Na_2SO_4 + V_2O_5$ Molten Salts," Coatings, vol. 9, no. 6: 351, 2019. https://doi.org/10.3390/coatings9060351

[9] W. Fang, T.Y. Cho, J.H. Yoon, K.O. Song, S.K. Hur, S.J. Youn, H.G. Chun, "Processing optimization, surface properties and wear behavior of HVOF spraying WC– CrC–Ni coating," Journal of Materials Processing Technology, vol. 209, pp. 3561-3567, 2009. https://doi.org/10.1016/j.jmatprotec.2008.08.024

[10] S. Choudhary, A. Islam, B. Mukherjee, J. Richter, T. Arold, T. Niendorf, A. K. Keshri, "Plasma sprayed Lanthanum zirconate coating over additively manufactured carbon nanotube reinforced Ni-based Composite: Unique performance of thermal barrier coating system without bondcoat," Applied Surface Science, vol. 550, p. 149397, 2021, https://doi.org/10.1016/j.apsusc.2021.149397

[11] F. Kirbiyik, M.G. Gok, G. Goller, "Recent Developments on Al_2O_3-Based Thermal Barrier Coatings. In: Pakseresht, A., Amirtharaj Mosas, K.K. (eds) Ceramic Coatings for High-Temperature Environments," Engineering Materials. Springer, Cham., 2024, https://doi.org/10.1007/978-3-031-40809-0_4

[12] R. Donnini, A. Varone, A. Palombi, S. Spiller, P. Ferro, G. Angella, "High Energy Density Welding of Ni-Based Superalloys: An Overview," Metals, vol. 15, no. 1:30, 2025.https://doi.org/10.3390/met15010030

[13] B. Rottwinkel, C. Nölke, S. Kaierle, V. Wesling, "Crack Repair of Single Crystal Turbine Blades Using Laser Cladding Technology," Procedia CIRP, vol. 22, pp. 263-267, 2014.

[14] P. D. Enrique, T. Minasyan, E. Toyserkani, "Laser powder bed fusion of difficult-to-print γ′ Ni-based superalloys: A review of processing approaches, properties, and remaining challenges," Additive Manufacturing, 2025, vol. 106, 104811, 2025. https://doi.org/10.1016/j.addma.2025.104811

[15] D. Frunzaverde, G. Marginean, C. R. Ciubotariu, "Corrosion and Cavitation Performance of Flame-Sprayed NiCrBSi Composite Coatings Reinforced with Hard Particles," Crystals, vol. 14, no.12: 1078, 2024.

[16] J. Fiebig, E. Bakan, T. Kalfhaus, G. Mauer, O. Guillon, R. Vaßen, "Thermal Spray Processes for the Repair of Gas Turbine Components," Adv. Eng. Mater., vol. 22, no.6: 1901237, 2020. https://doi.org/10.1002/adem.201901237

[17] M. Nicolaus, K. Möhwald, H.J. Maier, "Thermally Sprayed Nickel-Based Repair Coatings for High-Pressure Turbine Blades: Controlling Void Formation during a Combined Brazing and Aluminizing Process," Coatings, vol. 11, no. 6: 725, 2021. https://doi.org/10.3390/coatings11060725

[18] M. Létang, S. Björklund, S. Joshi et al., "Repair of Single-Crystal CMSX-4 Using the High Velocity Air Fuel Process," J Therm Spray Tech, vol. 34, pp. 1489–1506, 2025. https://doi.org/10.1007/s11666-025-01944-2

[19] V. Venkatachalapathy, N.K. Katiyar, A. Matthews, J.L. Endrino, S.A. Goel, "Guiding Framework for Process Parameter Optimisation of Thermal Spraying," Coatings, vol. 13, no 4: 713, 2023. https://doi.org/10.3390/coatings13040713

[20] R. S. Antar, S. Y. Darweesh, F. W. Ridha, "Production of a double cermet coating to treatment of the turbine blades," Engineering Research Express, vol. 6, pp. 2631-8695, 2024.

[21] F. Fanicchia, D.A. Axinte, J. Kell, R. McIntyre, G. Brewster, A.D. Norton, "Combustion Flame Spray of CoNiCrAlY & YSZ coatings," Surface and Coatings Technology, vol. 315, pp. 546-557, 2017. https://doi.org/10.1016/j.surfcoat.2017.01.070

[22] X. Wang, M. Li, Y. Wang, C. Zhang, Z. Wen, "Creep Damage Repair of a Nickel-Based Single Crystal Superalloy Based on Heat Treatment," Metals, vol. 11, no. 4: 623, 2021. https://doi.org/10.3390/met11040623

[23] Y. V. Petrov, V. M. Samoilenko, O.A. Ratenko, E.V. Samoilenko, "Protective Coating for Restoring the Operability of Gas Turbine Engine Blades with Allowance for Their Service-Induced Damage," Russian Metallurgy (Metally), vol. 2024, pp. 1555-6255, 2024. https://doi.org/10.1134/S0036029524702483

[24] N. V. Abraimov, V. V. Lukina, A. Y. Ivanova, "Technology for the Deposition of Wear-Resistant Coatings on the Airfoil Shroud Platforms of GTE Turbine Blades," Russian Metallurgy (Metally), vol. 2019, pp. 1555-6255, 2019. https://doi.org/10.1134/S0036029519060028

[25] S. Choudhary, V. Gaur, "Study of New Generation Thermal Barrier Coatings for High-Temperature Applications. In: Verma, A., Sethi, S.K., Ogata, S. (eds) Coating Materials. Materials Horizons: From Nature to Nanomaterials. Springer, Singapore, 2023. https://doi.org/10.1007/978-981-99-3549-9_15

[26] R. Rachida, E. K. Bachir, D. Fabienne, V. Vronique, D. Dorian, "Wear Performance of Thermally Sprayed NiCrBSi and NiCrBSi-WC Coatings Under Two Different Wear Modes," J. Mater. Environ. Sci., vol. 8, pp. 4550-4559, 2017. https://doi.org/10.26872/JMES.2017.8.12.480

[27] U. Harish, M. Mruthunjaya, R.R. Chakule, et al. "Effect of cobalt variation on microstructural and erosion performance of HVOF-sprayed WC–Co-Cr-Ni hard-faced coatings," J Mater. Sci: Mater Eng, vol. 20, no. 73, 2025. https://doi.org/10.1186/s40712-025-00264-1

[28] M. Mihoob, H. Mohammed H., T. Badri et al., "Optimal Process Parameters for a Thermal-Sprayed Molybdenum-Reinforced Zirconium Diboride Composite on a Dummy Substrate," Energies, vol. 15, no. 9415, 2022.

[29] M. Mrdak, "Microstructure and mechanical properties of nickel-chrome-bor-silicon layers produced by the atmospheric plasma spray process," Military Technical Courier, vol. 60, pp. 183-200, 2012. 10.5937/vojtehg1201183M.

[30] A. Dmitrieva, O. Klimova-Korsmik, M. Gushchina, R. Korsmik, G. Zadykyan, S. Tukov, "Effect of the Laser Cladding Parameters on the Crack Formation and Microstructure during Nickel Superalloy Gas Turbine Engines Repair," Metals, vol. 13, no. 2: 393, 2023. https://doi.org/10.3390/met13020393

[31] M. Li, K. Huang, X. Yi, "Crack Formation Mechanisms and Control Methods of Laser Cladding Coatings: A Review," Coatings, vol. 13, no. 6: 1117, 2023. https://doi.org/10.3390/coatings13061117.